CHEMISTRY
A EUROPEAN JOURNAL

DOI: 10.1002/chem.200801300

Polymerizing Cluster Helicates into High-Connectivity Networks

Shun-Ze Zhan, Mian Li, Jin-Zhang Hou, Jia Ni, Dan Li,* and Xiao-Chun Huang*[a]

Abstract: Solvothermal reactions of Cu^{II} salts and 3,5-bis(4-pyridyl)pyrazole (H**L**) under various conditions gave three different types of crystalline compound, namely $[Cu_2(Cu_5L_6)]BF_4\cdot5H_2O$ (**1a**), $[Cu_2(Cu_5L_6)]ClO_4\cdot5H_2O$ (**1b**), and $[Cu_7(CN)_2(Cu_5L_6)_2][BF_4]_3$ (**2**). **1a** and **b** were obtained in ethanol and $NH_3\cdot H_2O$, whereas **2** was obtained in methanol and $NH_3\cdot H_2O$. The three complexes were constructed by incorporating new pentanuclear copper(I) pyrazolate bis(triple helical) cluster helicates (Cu_5L_6) as the second building units (SBUs), in which as many as twelve 4-pyridyl N atoms are available for further coordination and construction of high-connectivity topological networks. In **1a** and **b**, seven 4-pyridyl N atoms are linked to three three-coordinated Cu^I atoms and four four-coordinated Cu^I atoms, which results in 3,4,7-connected networks. In **2**, as many as eleven 4-pyridyl N atoms coordinate to eleven Cu^I atoms, which results in a 4,10-connected topological network. The increasing connectivity of the cluster nodes in **2** is closely related to the in situ-formed CN^- anion bridge around the periphery of the pentanuclear cluster helicates. The luminescenct properties of these compounds were also investigated.

Keywords: cluster compounds · coordination polymers · copper · helical structures · high connectivity · pyrazole

Introduction

First introduced by J.-M. Lehn in 1987,[1] over the last two decades the field of multistranded helicates has been seeding chemists' everlasting desire to target appealing metallo-supramolecular edifices with helical archetypes, the potential functions of which are observed at the microscopic level.[2,3] A conventional strategy that utilizes long and twistable ligands for the construction of helicates has proved to be reliable.[4] However, this synthetic algorithm encounters challenges in pursuit of multimetallic helicates (tetranuclear or more), in which the metal centers are disposed in a polyhedral mode, namely, cluster helicates.[5]

Cluster helicates, a term coined by Bermejo et al. in 2005,[5] have formed an emerging concept that involves compound types which combine the structural characters of helicates and clusters. In the sporadically documented examples of multimetallic helicates with polyhedral central cores,[6] few of them displayed significant metal–metal interactions and failed to exemplify genuine cluster helicates. In contrast with the strategy of judicious selection of dianionic helicand ligands,[5,6c] an anionic pyrazolate derivate with a typical edge-bridging mode[7] was shown to give an intriguing example of a pentanuclear M_5L_6 cluster helicate.[8] Recently, we utilized a similar cluster helicate (**A**; Figure 1, left) as a template to fabricate helical coordination polymers through a sulfur transformation reaction, and successfully implemented supramolecular helix-to-helix induction.[9]

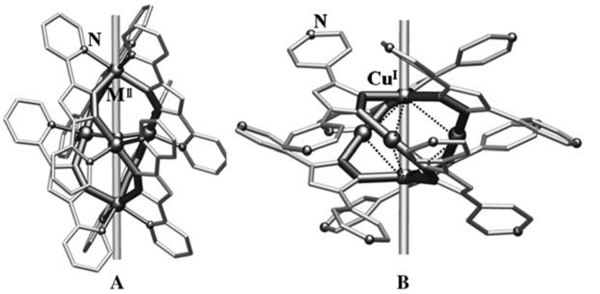

Figure 1. Two types of pentanuclear copper(I) pyrazolate bis(triple helical) cluster helicates with Λ (*M*) conformation. Left: Cluster helicate **A**,[8,9] constructed from the 3,5-bis(2-pyridyl)pyrazolate ligand; right: cluster helicate **B**, constructed from the 3,5-bis(4-pyridyl)pyrazolate ligand.

---

[a] S.-Z. Zhan, M. Li, J.-Z. Hou, J. Ni, Prof. D. Li, Dr. X.-C. Huang
Department of Chemistry
Shantou University
Guangdong 515063 (China)
Fax: (+86) 754-290-2767
E-mail: dli@stu.edu.cn
xchuang@stu.edu.cn

Supporting information for this article is available on the WWW under http://dx.doi.org/10.1002/chem.200801300.

In an attempt to polymerize cluster compounds into coordination polymers,[10] an analogous ligand, 3,5-bis(4-pyridyl)-pyrazole (**HL**),[11] was synthesized in place of 3,5-bis(2-pyridyl)pyrazole, which was used to prepare cluster helicate **A**[9]. A rational consideration indicated that the 4-pyridyl substituents might serve as bridging spacers for constructing extended architectures in place of the terminal chelating groups (2-pyridyl substituents) in **A** (Figure 1, left). Assuming that the configuration of the M_5L_6 central core remains unchanged by taking advantage of the edge-bridging mode of the pyrazolate groups, and the 4-pyridyl substituents stay uncoordinated, it is apparent that an M^I metal ion with a low coordination number, other than the M^{II} (e.g., Ni^{II} and Zn^{II}) metal ions used in the preparation of **A**, would be required to fulfill the coordination balance between the metal atoms and ligands.[5] By taking the above into consideration, we report herein a new M_5L_6 cluster helicate (**B**; Figure 1, right), which acts as a secondary building unit (SBU) that has 4-pyridyl vacant sites for further coordination to construct high-connectivity coordination networks.[12]

Results and Discussion

Synthesis: Solvothermal reactions of Cu^{II} salts and **HL** in various conditions gave three different types of crystalline products, $[Cu_2(Cu_5L_6)]BF_4{\cdot}5H_2O$ (**1a**), $[Cu_2(Cu_5L_6)]ClO_4{\cdot}5H_2O$ (**1b**), and $[Cu_7(CN)_2(Cu_5L_6)_2][BF_4]_3$ (**2**). **1a** and **b** were obtained as yellowish transparent prismatic crystals in ethanol and $NH_3{\cdot}H_2O$ at 140–160 °C, whereas **2** was separated as yellowish transparent columnular crystals in methanol and $NH_3{\cdot}H_2O$ at 160 °C (Figure S1 in the Supporting Information). The in situ reduction of Cu^{II} to Cu^I was broadly confirmed by the solvothermal reactions.[13]

The infrared spectrum of **2** shows bands at $\tilde{\nu}=2100\ cm^{-1}$, which is attributed to the stretch vibration of C≡N. In fact, many other Cu^I complexes based on **HL** or related ligands contain in situ-formed cyanide anions from methanol and $NH_3{\cdot}H_2O$ under solvothermal conditions, which will be reported in further publications. Herein we suggest the rationalized pathway for the formation of the cyanide anions, as follows:

$$CH_3OH \rightarrow HCHO \rightarrow CH_2{=}NH \rightarrow HCN \rightarrow CN^-$$

There are previous literature reports of the in situ formation of cyanide anions from HCHO and $NH_3{\cdot}H_2O$ via the imine ($CH_2{=}NH$) intermediate.[14] We attempted to capture the HCHO and $CH_2{=}NH$ intermediates in the filtrate by performing GC–MS measurements. Unfortunately, there was no observable peak attributable to the HCHO or $CH_2{=}NH$ intermediates, probably because of their low concentrations in the filtrate and the difficulty of distinguishing their peaks from the peaks of N_2 from air or the CH_3OH solvent.

Pentanuclear Cu_5L_6 cluster helicate SBU: X-ray crystallography revealed that **1a**,**b** (isostructures, tetrafluoroborate and perchlorate, respectively) and **2** (tetrafluoroborate) are constructed by similar pentanuclear copper(I) pyrazolate cluster **B** (Figure 1, left). In each cluster, five Cu^I atoms are arranged on the five vertices of a squashed trigonal-bipyramidal polyhedron. Ideally, the distances of six $Cu_{ax}\cdots Cu_{eq}$ (edge-bridged by deprotonated **L** ligands; ax = axial, eq = equitorial) would be equal, and there would be a C_3 axis that passed through the Cu1 and Cu2, and thus the cluster would belong to D_3 point group. However, **1a**,**b** and **2** crystallize in the $P2_1/c$ and $C2/c$ (monoclinic, with lower symmetry than trigonal) space groups, respectively. The $Cu_{ax}\cdots Cu_{eq}$ distances are much shorter than $Cu_{eq}\cdots Cu_{eq}$ distances (Table 1), which indicates stronger Cu⋯Cu interactions in the axis orientation than in the equator orientation. The two Cu^I atoms along the axis (Cu1 and Cu2) are roughly planar three-coordinated, whereas the three Cu^I atoms on the equator (Cu3, Cu4, and Cu5) are approximately linearly coordinated. Six **L** ligands are located on the edge of the trigonal bipyramid, and arranged in a bis(triple helical) shape[6a,8,9] around the central pentanuclear Cu^I cluster core through pyrazolate edge-bridging of two adjacent Cu^I atoms. Accordingly, this M_5L_6 (**B**) unit can be described as a cluster helicate in which the metal cluster defines the helical axis.[5] It is clear that cluster helicate **B** exhibits two conformations (Δ and Λ, or *P* and *M*)[2a,15] in light of the helical chirality (Figures S2 and S3 in the Supporting Information). The construction of cluster helicate **B**, which is stabilized by significant metal–metal interactions,[16] is distinct from previously reported cluster helicates and **A**,[6,8] and provides a unique example of a genuine multimetallic cluster helicate.

Table 1. Cu–Cu distances of pentanuclear cluster units.

Cu interaction		Distance [Å]		
		1a	**1b**	**2**
Cu_{ax}–Cu_{eq}	Cu1–Cu3	3.1070	3.1255	2.9123
	Cu1–Cu4	3.1993	3.2199	3.0900
	Cu1–Cu5	2.8815	2.8822	3.1436
	Cu2–Cu3	2.9987	3.0053	2.9571
	Cu2–Cu4	3.2439	3.2411	3.0457
	Cu2–Cu5	2.9806	2.9846	3.1500
	(average)	(3.0685)	(3.0764)	(3.0498)
Cu_{eq}–Cu_{eq}	Cu3–Cu4	3.9434	3.9505	3.7373
	Cu4–Cu5	3.7752	3.7768	3.7562
	Cu3–Cu5	3.9678	3.9555	4.0381
	(average)	(3.8955)	(3.8943)	(3.8439)

High-connectivity cluster-helicate-based networks: As mentioned above, the twelve 4-pyridyl nitrogen atoms from six **L** ligands are available for further coordination. Cluster helicate **B** may act as a SBU, with the connectivity number expected to be as high as twelve. However, the steric hindrance might more or less reduce the connectivity in the self-assembly processes.

In **1a** and **b**, only seven of the twelve pyridyl N atoms are linked to three three-coordinated Cu^I atoms (Cu6, Cu6A, Cu6B) and four four-coordinated Cu^I atoms (Cu7, C7C, Cu7D, Cu7E), respectively, and the five remaining pyridyl N atoms are vacant (Figure 2a). Only one **L** ligand acts as a tetradentate ligand and the other five ligands are tridentate. Through these seven Cu^I atoms, each cluster helicate **B** is connected to eleven others surrounding it (Figure S4a in the Supporting Information), polymerizing each other into a complicated 3D coordination network that includes one counterion (BF_4^- for **1a** and ClO_4^- for **1b**) and five guest water molecules per cluster unit. The occupied space of each M_5L_6 cluster is about 2000 Å^3 (each cell unit contains four M_5L_6 clusters). Left- (Λ or *M*) and right-handed (Δ or *P*) triple-stranded helicate enantiomers exist, which arrange in an alternately homochiral *PPMM* (ΔΔΛΛ) bilayer packing fashion along the *c* axis (Figure 2c) through symmetry operations, which result in racemic compounds, consistent with the central symmetry space groups of **1a** and **b**. Topologically, the pentanuclear cluster helicates in **1a** and **b** act as 7-connected nodes (Figure S4a in the Supporting Information), and the seven Cu^I atoms around the cluster can be envisioned as 3- and 4-connected nodes. Therefore, **1a** and **b** exhibit 3,4,7-connected networks with the Schläfli symbol of $(4^3)(4^4{\cdot}6^2)(4^7{\cdot}6^{11}{\cdot}8^3)$,[12a] which is composed of two subnets that share these cluster nodes. One is a 2D subnet constructed from the three-coordinated Cu^I atoms (Cu6, Cu6A, Cu6B) connecting these clusters, the other is a 3D $(4^2{\cdot}6^3{\cdot}8)$ subnet (sra net; i.e., its structure is analogous to the aluminum network in $SrAl_2$)[17] constructed from the four-coordinated Cu^I atoms (Cu7, C7C, Cu7D, Cu7E) that connect these cluster nodes (Figure 3a and Figure S5 in the Supporting Information).

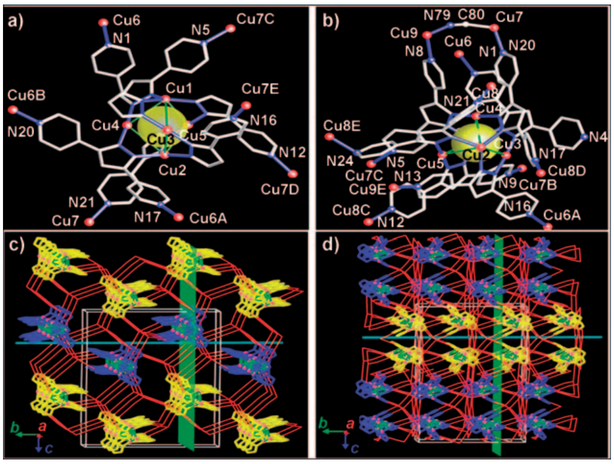

Figure 2. Peripheral environments of the pentanuclear copper(I) pyrazolate cluster helicate B in a) **1a** and **b**, symmetry codes: A: $x, -y+\frac{1}{2}\ z+\frac{1}{2}$; B: $-x+2, -y+1, -z+1$; C: $x, -y+\frac{1}{2}, z-\frac{1}{2}$; D: $-x+1, y-\frac{1}{2}, -z+\frac{3}{2}$; E: $-x+2, y-\frac{1}{2}, -z+\frac{3}{2}$; and b) **2** (vacant pyridyls are omitted for clarity), symmetry codes: A: $x-\frac{1}{2}, y-\frac{1}{2}, z$; B: $-x+\frac{1}{2}, y-\frac{1}{2}, -z+\frac{1}{2}$; C: $x+\frac{1}{2}, y-\frac{1}{2}, z$; D: $-x-\frac{1}{2}, -y+\frac{1}{2}, -z$; E: $-x+\frac{1}{2}, -y+\frac{1}{2}, -z$). Packing arrangements of left- (yellow) and right-handed (blue) cluster helicates along the *a* axis in c) **1a** and **b** and d) **2**, which show the 2_1 screw axis in **1a** and **b** and the C_2 axis in **2** (——), the glide reflection (green plane, $b=\frac{1}{4}$ crystallography planes, the glide vector $c=\frac{1}{2}$ for **1a** and **b** and $n=\frac{1}{2}$ for **2**). Anions and water molecules are omitted and pyridyls are simplified as red bonds for clarity.

In **2**, as many as eleven pyridyl N atoms coordinate with eleven Cu^I atoms. Four of the eleven Cu^I atoms (Cu6, Cu7, Cu8, Cu9) are symmetry dependent. Cu6 and Cu8 are coordinated by four pyridyl N atoms from four clusters, respectively. Cu6 atoms are located at *C*2 rotation axis (Figure S3c in the Supporting Information), and each Cu6 atom is coordinated by two pairs of symmetry-related N1 and N16 atoms (Figure 2b), whereas each Cu8 is coordinated by four symmetry-independent pyridyl N atoms (N21, N12, N17, N24, Figure 2b). In contrast, the Cu7 and Cu9 atoms are coordinated by three pyridyl N atoms (N5, N9, N20) and two pyridyl N atoms (N8, N13) from different clusters and a cyanide anion, respectively (Figure 2b). Only one **L** acts as a tridentate ligand (the N4 atom is vacant), the others are tetradentate. It is worth noting that Cu8F deviates severely from the plane of N24 pyridyl ring (the angle between the bond and the plane is 142°), and the distance between Cu8F and N24 is 2.1823 Å, much longer than the other Cu–N bonds, which indicates the interaction between Cu8F and N24 is much weaker. Through these eleven Cu^I atoms, each cluster is connected to sixteen others around it (Figure S4b), also polymerizing each other into a complicated 3D coordination network that contains one and a half counteranions (BF_4^-) per cluster unit but no solvent molecules. The occupied space of each M_5L_6 cluster is about 2000 Å^3 (each cell

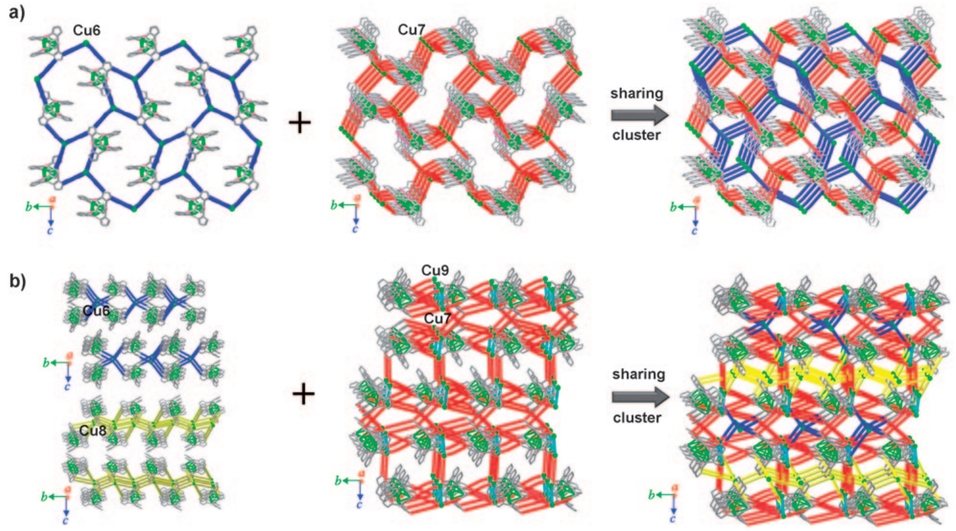

Figure 3. Schematic representation of the formation of topological networks of a) **1a** and **b** and b) **2** by various subnets with cluster sharing nodes.

unit contains eight M_5L_6 clusters), which is similar to **1a** and **b**. The different handedness packing fashion of the cluster helicates in **2** is similar to the alternately *PPMM* (ΔΔΛΛ) fashion of **1a** and **b** (Figure 2d). By denoting Cu7 and Cu9 bridged by cyanide anion as a 4-connected node and one cluster as a 10-connected node (Figure S4b in the Supporting Information), **2** can be rationalized as a 4,10-connected net with a Schläfli symbol of $(4^3\cdot6^3)(4^5\cdot6)(4^5\cdot6)(4^{18}\cdot6^{22}\cdot8^5)$[12a] The complicated 3D network is composed of three subnets that share these cluster nodes; two types of 2D subnet through Cu6 and Cu8 that connect these cluster nodes and one 3D 4-connected subnet with a Schläfli symbol of $(4^3\cdot6^2\cdot8)$, constructed from Cu7/Cu9 atoms that connect these clusters (Figure 3b and Figure S6 in the Supporting Information).To our knowledge, such a topology that contains 10-connected nodes is rarely encountered.

In the formation of the highly connected network of **2**, the in situ-formed CN^- anions play a key role by acting as linear bridges that connect Cu^I atoms (Cu7 and Cu9) around the periphery of the pentanuclear cluster helicates, but not between these clusters (Figure 2b), which thus leads to the increasing connectivity of the cluster nodes (from seven connections in **1a** and **b** to ten in **2**). The similarly occupied space of each M_5L_6 cluster in **1a**,**b** and **2** indicates that the existence of CN^- anions in **2** did not increase the intercluster distances. Therefore, the most likely reason that CN^- increases the connectivity is that its negative charge favors the aggregation of more positive Cu^I cations around the periphery of the pentanuclear cluster helicates to form more Cu–N bonds, and thus lead to the higher connectivity of the cluster nodes.

Luminescence properties: The photoluminescence of these Cu^I complexes were also investigated (Figure 4). Upon irradiation with light of $\lambda = 390$ nm, the three complexes show orange photoluminescence properties with broad emission peaks ($\lambda_{em,max} = 600$, 596, and 580 nm for **1a**,**b**, and **2**, respectively) at room temperature. We tentatively assigned the emissions as originating from the metal-centered ^{3}[MC] or metal–metal bond to ligand charge transfer ^{3}[MMLCT] excited states,[18] which is reasonable because various weak Cu···Cu interactions are obvious in the pentanuclear Cu^I cluster (Table 1). The blueshift of **2** is coincident with the fact that the Cu···Cu distances are shorter in **2** than in **1a**,**b**.

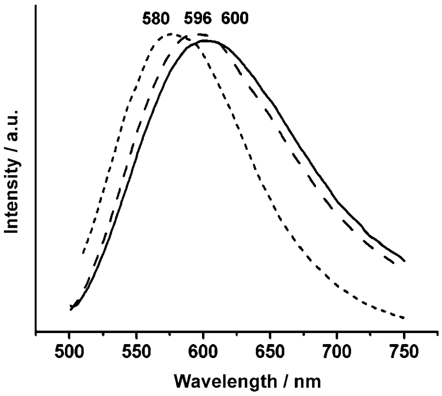

Figure 4. Solid-state emission spectra of **1a** (——), **1b** (– – –), and **2** (-----) at room temperature.

Conclusion

Herein, we have introduced a new pentanuclear Cu_5L_6 bis-(triple helical) cluster helicate, which is incorporated in two types of high-connectivity coordination networks. For the first time, this work implements the polymerization of cluster helicate cores into coordination polymers by taking advantage of the edge-bridging mode of the pyrazolate ligand and by reducing the coordination number of the metal center. We believe that this work offers valuable insights into both the construction of high-connectivity cluster-based topological networks, and also the functionalization of helical cluster cores toward the construction of functional metallosupramolecular edifices with intriguing physical properties.

Experimental Section

Materials and Physical Measurements: Commercially available reagents (Alfa Aesar) were used as received, without further purification. 3,5-Bis(4-pyridyl)pyrazole (abbreviated to **HL**) was prepared according to our previous literature procedure.[11] Infrared spectra were obtained with KBr disks by using a Nicolet Avatar 360 FTIR spectrometer in the range of $\tilde{\nu} = 4000$–400 cm^{-1}; abbreviations used for the IR bands are w = weak, m = medium, b = broad, vs = very strong. Elemental analyses of C, H, and N percentages were determined by using a Perkin–Elmer 2400C elemental analyzer. X-Ray power diffraction (XRPD) experiments were performed by using a D8 Advance X-Ray diffractometer. Steady-state photoluminescence spectra were performed by using an Edinburg FLS920 spectrometer equipped with a continuous Xe900 Xenon lamp. In all cases, single-crystalline samples were used for the photoluminescence measurements.

Synthesis of $[Cu_2(Cu_5L_6)]BF_4\cdot5H_2O$ (1a): 5 drops of aqueous NH_3 were added to a solution of $\mathbf{HL}\cdot3H_2O$ (55.2 mg, 0.2 mmol) and $Cu(BF_4)_2\cdot6H_2O$ (207.0 mg, 0.6 mmol) in ethanol (10 mL), the mixture was sealed in a 15 mL Teflon-lined reactor and heated in an oven at 160 °C for 72 h, and then slowly cooled to RT at a rate of 3 °C/30 min. The title compound was obtained as yellow block crystals (yield = 27.0 mg, 41.55 % based on **HL**). IR (KBr disc): 3117 (w), 3051 (w), 1605 (vs), 1470 (m), 1409 (m), 1213 (m), 1050–1100 (b), 837 (m), 722 cm^{-1} (m); elemental analysis calcd (%) for $C_{78}H_{64}N_{24}Cu_7BF_4O_5$: C 48.02, H 3.28, N 17.24; found: C 48.00, H 3.28, N 17.20.

Synthesis of $[Cu_2(Cu_5L_6)](ClO_4)\cdot5H_2O$ (1b): The procedure was analogous to that of **1a**, except that $Cu(BF_4)_2\cdot6H_2O$ was replaced by $Cu(ClO_4)_2\cdot6H_2O$ (222.3 mg, 0.6 mmol). The title compound was obtained as yellow block crystals (yield = 20.5 mg, 31.35 % based on **HL**). IR (KBr disc): 3125 (w), 3035 (w), 1605 (vs), 1470 (m), 1417 (m), 1221 (m), 1080–1120 (b), 833 (m), 722 cm^{-1} (m); elemental analysis calcd (%) for $C_{78}H_{64}N_{24}Cu_7ClO_9$: C 47.71, H 3.26, N 17.12; found: C 48.01, H 3.20, N 17.22.

Synthesis of $[Cu_7(CN)_2(Cu_5L_6)_2](BF_4)_3$ (2): The procedure was analogous to that of **1a**, except that ethanol was replaced by methanol (10 mL). The title compound was obtained as two types of yellow crystals, that is, block and prismatic, that were separated manually (yield = 8.5 and 15.6 mg, 13.08 and 23.12 % based on **HL** for **1a** and **2**). IR (KBr disc): 3121 (w), 3043 (w), 2100 (m), 1605 (vs), 1470 (m), 1413 (m), 1217 (m), 1050–1100 (b), 837 (m), 723 cm^{-1} (m); elemental analysis calcd (%) for

$C_{158}H_{108}N_{50}Cu_{17}B_3F_{12}$: C 46.84, H 2.67, N 17.29; found: C 47.02, H 2.61, N 17.20.

Crystal strucure determination: Data collection was performed by using a Bruker Smart Apex CCD diffractometer ($Mo_{K\alpha}$ radiation, $\lambda = 0.71073$ Å) with frames with 0.3° oscillation ($4.56 \leq 2\theta \leq 50°$). The structure was solved by using direct methods, and all nonhydrogen atoms were refined anisotropically by the full-matrix least-square method on F^2 by using the SHELXTL program (G. M. Sheldrick, SHELXTL v. 6.10, Bruker Analytical Instrumentation, Madison, Wisconsin (USA), **2000**). The C/N atoms of CN^- in **2** were undistinguishable, and were refined with a 50% probability of being C or N and were assigned randomly as C or N atoms. The hydrogen atoms were located from different maps and refined with isotropic temperature factors (see the Supporting Information). CCDC-684126 (**1a**), -684127 (**1b**), and -684128 (**2**) contain the supplementary crystallographic data for this paper. These data can be obtained free of charge from The Cambridge Crystallographic Data Centre via www.ccdc.cam.ac.uk/data_request/cif. Crystal and structure refinement data for **1a**,**b**, and **2** are summarized in Table 2.

Table 2. Crystal data and structure refinement for **1a**,**b** and **2**.

	1a	**1b**	**2**
formula	$C_{78}H_{64}N_{24}$-$Cu_7BF_4O_5$	$C_{78}H_{64}N_{24}$-Cu_7ClO_9	$C_{316}H_{216}N_{100}$-$Cu_{34}B_6F_{24}$
M_r	1949.12	1961.76	8095.11
crystal system	monoclinic	monoclinic	monoclinic
space group	$P2_1/c$	$P2_1/c$	$C2/c$
a [Å]	11.4602(6)	11.4070(10)	15.5804(8)
b [Å]	22.8607(12)	22.7362(19)	25.5721(13)
c [Å]	30.7886(16)	30.981(3)	40.857(2)
α[°]	90	90	90
β [°]	96.0170(10)	96.769(2)	96.3970(10)
γ[°]	90	90	90
V [Å^3]	8021.8(7)	7978.9(12)	16177.2(14)
Z	4	4	2
ρ_{calcd} [g cm^{-3}]	1.614	1.633	1.662
μ [mm^{-1}]	1.897	1.937	1.132
reflns coll.	41399	41377	42301
unique reflns	14134	14053	14252
R_{int}	0.0537	0.0443	0.0539
$R1$ [$I > 2\sigma(I)$][a]	0.0598	0.0509	0.0671
$wR2$ [$I > 2\sigma(I)$][b]	0.1539	0.1343	0.1874
$R1$ (all reflns)	0.0979	0.0872	0.1044
$wR2$ (all reflns)	0.1749	0.1577	0.2193

[a] $R1 = \Sigma(||F_o| - |F_c||)/\Sigma|F_o|$. [b] $wR_2 = [\Sigma_w(F_o^2 - F_c^2)^2/\Sigma_w(F_o^2)^2]^{1/2}$.

Acknowledgement

This work was financially supported by the National Natural Science Foundation of China (grant nos. 20571050 and 20771072) and the Natural Science Foundation of Guangdong Province of China (no. 06027203).

---

[1] a) R. C. Scarrow, D. L. White, K. N. Raymond, *J. Am. Chem. Soc.* **1985**, *107*, 6540–6546; b) J.-M. Lehn, A. Rigault, J. Siegel, J. Harrowfield, B. Chevrier, D. Moras, *Proc. Natl. Acad. Sci. USA* **1987**, *84*, 2565; c) E. C. Constable, *Nature* **1990**, *346*, 314–315; d) J.-M. Lehn, *Supramolecular Chemistry: Concepts and Perspectives*, Wiley-VCH, Weinheim, **1995**.

[2] For reviews, see: a) C. Piguet, G. Bernardinelli, G. Hopfgartner, *Chem. Rev.* **1997**, *97*, 2005–2062; b) J.-C. G. Bünzli, C. Piguet, *Chem. Rev.* **2002**, *102*, 1897–1928; c) C. Piguet, M. Borkovec, J. Hamacek, K. Zeckert, *Coord. Chem. Rev.* **2005**, *249*, 705–726.

[3] For reviews, see: a) M. Albrecht, *Chem. Soc. Rev.* **1998**, *27*, 281–287; b) M. Albrecht, *Chem. Eur. J.* **2000**, *6*, 3485–3489; c) M. Albrecht, *Chem. Rev.* **2001**, *101*, 3457–3497; d) M. Albrecht, *Angew. Chem.* **2005**, *117*, 6606–6609; *Angew. Chem. Int. Ed.* **2005**, *44*, 6448–6451.

[4] For examples, see: a) J. Hamacek, S. Blanc, M. Elhabiri, E. Leize, A. V. Dorsselaer, C. Piguet, A.-M. Albrecht-Gary, *J. Am. Chem. Soc.* **2003**, *125*, 1541–1550; b) Z. Grote, S. Bonazzi, R. Scopelliti, K. Severin, *J. Am. Chem. Soc.* **2006**, *128*, 10382–10383; c) T. Kreickmann, C. Diedrich, T. Pape, H. V. Huynh, S. Grimme, F. E. Hahn, *J. Am. Chem. Soc.* **2006**, *128*, 11808–11819; d) M. Albrecht, S. Dehn, R. Fröhlich, *Angew. Chem.* **2006**, *118*, 2858–2860; *Angew. Chem. Int. Ed.* **2006**, *45*, 2792–2794; e) J. Xu, K. N. Raymond, *Angew. Chem.* **2006**, *118*, 6630–6635; *Angew. Chem. Int. Ed.* **2006**, *45*, 6480–6485.

[5] M. R. Bermejo, A. M. González-Noya, R. M. Pedrido, M. J. Romero, M. Vázquez, *Angew. Chem.* **2005**, *117*, 4254–4259; *Angew. Chem. Int. Ed.* **2005**, *44*, 4182–4187.

[6] a) R. W. Saalfrank, N. Löw, S. Trummer, G. M. Sheldrick, M. Teichert, D. Stalke, *Eur. J. Inorg. Chem.* **1998**, 559–563; b) P. N. W. Baxter, J.-M. Lehn, G. Baum, D. Fenske, *Chem. Eur. J.* **2000**, *6*, 4510–4517; c) M. Bera, G. Aromí, W. T. Wong, D. Ray, *Chem. Commun.* **2006**, 671–673.

[7] For examples, see: a) A. L. Gavrilova, B. Bosnich, *Chem. Rev.* **2004**, *104*, 349–384; b) G. A. Ardizzoia, G. L. Monica, S. Cenini, M. Moret, N. Masciocchi, *J. Chem. Soc. Dalton Trans.* **1996**, 1351–1357; c) M. H. W. Lam, S. T. C. Cheung, K.-M. Fung, W.-T. Wong, *Inorg. Chem.* **1997**, *36*, 4618–4619; d) J. He, Y.-G. Yin, T. Wu, D. Li, X.-C. Huang, *Chem. Commun.* **2006**, 2845–2847; e) J.-X. Zhang, J. He, Y.-G. Yin, M.-H. Hu, D. Li, X.-C. Huang, *Inorg. Chem.* **2008**, *47*, 3471–3473; f) J.-P. Zhang, S. Horike, S. Kitagawa, *Angew. Chem.* **2007**, *119*, 907–910; *Angew. Chem. Int. Ed.* **2007**, *46*, 889–892; g) J.-P. Zhang, S. Kitagawa, *J. Am. Chem. Soc.* **2008**, *130*, 907–917.

[8] K. Yoneda, K. Adachi, K. Nishio, M. Yamasaki, A. Fuyuhiro, M. Katada, S. Kaizaki, S. Kawata, *Angew. Chem.* **2006**, *118*, 5585–5587; *Angew. Chem. Int. Ed.* **2006**, *45*, 5459–5461.

[9] J.-Z. Hou, M. Li, Z. Li, S.-Z. Zhan, X.-C. Huang, D. Li, *Angew. Chem.* **2008**, *120*, 1735–1738; *Angew. Chem. Int. Ed.* **2008**, *47*, 1711–1714.

[10] For examples, see: a) D.-L. Long, P. Kögerler, L. J. Farrugia, L. Cronin, *Chem. Asian J.* **2006**, *1*, 352–357; b) J.-J. Zhang, H.-J. Zhou, A. Lachgar, *Angew. Chem.* **2007**, *119*, 5083–5086; *Angew. Chem. Int. Ed.* **2007**, *46*, 4995–4998; c) S. N. Semenov, A. Y. Rogachev, S. V. Eliseeva, C. Pettinari, F. Marchetti, A. A. Drozdov, S. I. Troyanov, *Chem. Commun.* **2008**, 1992–1994.

[11] S.-Z. Zhan, D. Li, X.-P. Zhou, X.-H. Zhou, *Inorg. Chem.* **2006**, *45*, 9163–9165.

[12] For examples, see: a) N. W. Ockwig, O. Delgado-Friedrichs, M. O'Keeffe, O. M. Yaghi, *Acc. Chem. Res.* **2005**, *38*, 176–182; b) R. J. Hill, D.-L. Long, N. R. Champness, P. Hubberstey, M. Schröder, *Acc. Chem. Res.* **2005**, *38*, 335–348; c) D. Li, T. Wu, X.-P. Zhou, R. Zhou, X.-C. Huang, *Angew. Chem.* **2005**, *117*, 4247–4250; *Angew. Chem. Int. Ed.* **2005**, *44*, 4175–4178; d) X.-M. Zhang, R.-Q. Fang, H.-S. Wu, *J. Am. Chem. Soc.* **2005**, *127*, 7670–7671; e) Q.-R. Fang, G.-S. Zhu, Z. Jin, M. Xue, X. Wei, D.-J. Wang, S.-L. Qiu, *Angew. Chem.* **2006**, *118*, 6272–6276; *Angew. Chem. Int. Ed.* **2006**, *45*, 6126–6130; f) X.-L. Wang, C. Qin, E.-B. Wang, Z.-M. Su, Y.-G. Li, L. Xu, *Angew. Chem.* **2006**, *118*, 7571–7574; *Angew. Chem. Int. Ed.* **2006**, *45*, 7411–7414; g) F. Nouar, J. F. Eubank, T. Bousquet, L. Wojtas, M. J. Zaworotko, M. Eddaoudi, *J. Am. Chem. Soc.* **2008**, *130*, 1833–1835.

[13] a) X.-M. Zhang, *Coord. Chem. Rev.* **2005**, *249*, 1201–1219; b) X.-M. Chen, M.-L. Tong, *Acc. Chem. Res.* **2007**, *40*, 162–170.

[14] a) F. B. Stocker, *Inorg. Chem.* **1991**, *30*, 1472–1475; b) F. B. Stocker, T. P. Staeva, C. M. Rienstra, D. Britton, *Inorg. Chem.* **1999**, *38*, 984–991.

[15] G. Seeber, B. E. F. Tiedemann, K. N. Raymond, *Top. Curr. Chem.* **2006**, *265*, 147–183.

[16] a) G. Yang, R. G. Raptis, *Chem. Commun.* **2004**, 2058–2059; b) J.-P. Zhang, Y.-Y. Lin, X.-C. Huang, X.-M. Chen, *J. Am. Chem. Soc.* **2005**, *127*, 5495–5506.

[17] a) L. S. Reddy, B. R. Bhogala, A. Nangia, *CrystEngComm* **2005**, *7*, 206–209; b) Z.-R. Qu, H. Zhao, X.-S. Wang, Y.-H. Li, Y.-M. Song, Y.-J. Liu, Q. Ye, R.-G. Xiong, B. F. Abrahams, Z.-L. Xue, X.-Z. You, *Inorg. Chem.* **2003**, *42*, 7710–7712.

[18] a) P. C. Ford, E. Cariati, J. Bourassa, *Chem. Rev.* **1999**, *99*, 3625–3647; b) V. W.-W. Yam, K. K.-W. Lo, *Chem. Soc. Rev.* **1999**, *28*, 323–334.

Received: June 29, 2008